*Int. J. Solids Structures* Vol. 24, No. 9, pp. 937–945, 1988
Printed in Great Britain.

0020–7683/88 $3.00 + .00


# ELASTIC–PLASTIC RESPONSE OF POROUS METALS UNDER TRIAXIAL LOADING

K. T. KIM
Department of Mechanical Engineering, Pohang Institute of Science and Technology, Pohang 790-600, Korea

(*Received* 15 *June* 1987)

**Abstract**—Special constitutive equations are presented to describe the elastic–plastic response of porous metals. Employing a simple yield function, the theory is compared with experimental results for porous tungsten. Responses under hydrostatic compression and uniaxial strain compression are considered.

## 1. INTRODUCTION

Considerable effort has been devoted to the development of constitutive theories for the mechanical response of porous solids undergoing elastic–plastic deformation. This trend is apparent in such research areas as powder metallurgy, geotechnical engineering, shock wave physics, and ceramic engineering.

The volumetric deformation of porous materials has been described by various methods ranging from simple phenomenological modeling to micromechanical modeling. The pore collapse models which use spherical pores may be at this time the most powerful and convenient (Torre, 1948; Mackenzie, 1950; Carroll and Holt, 1972, 1973; Carroll and Kim, 1984; Kim and Carroll, 1987).

The response of porous materials under general three-dimensional loading conditions is quite complicated and may exhibit strong coupling between volumetric and deviatoric effects. Johnson and Green (1976) discussed some of these effects, such as shear enhanced compaction (i.e. that the role of shear stress is to enhance the amount of volume compaction as compared to the purely hydrostatic behavior). Curran and Carroll (1979) carried out the spherical pore model calculations by using a finite element method to account for the deviatoric effects. Their numerical solutions showed good agreement with experimental data of porous metals and porous rocks.

An alternative approach to the development of constitutive theories for porous solids is macroscopic elastoplasticity. In this approach a porous solid is treated as a homogeneous continuum with a porosity parameter $\phi$ which is related to plastic strain.

Several yield functions for porous solids have been proposed. Green (1972), Gurson (1977), and de Boer and Kowalski (1983) obtained yield functions which are based on approximate analytical solutions for a rigid–perfectly plastic hollow sphere. Kuhn and Downey (1971) and Shima and Oyane (1976) proposed empirical yield functions.

In this paper special constitutive equations are presented for elastic–plastic deformation of porous metals. The elastic deformation is described by the generalized Hooke's law with the effective elastic moduli of a porous metal. The elastic–plastic deformation is described by an empirical yield function for a porous metal and a constitutive theory which has been developed by Naghdi and co-workers (Green and Naghdi, 1965, 1966; Naghdi and Trapp, 1975a, b; Casey and Naghdi, 1981, 1984a, b). A strain space formulation is employed in this paper because there is some ambiguity in a stress space formulation; for instance, the conditions $f = 0$ and $\hat{f} < 0$ correspond both to unloading and softening during loading (Casey and Naghdi, 1983). In any region of hardening, the loading conditions of the stress space and strain space formulations imply one another. However, in regions of softening and perfectly plastic behavior, the conditions in the two formulations do not imply one another. The yield function presented in this paper has a simpler form and gives a better agreement for real porous metals than those proposd by Green (1972) and by Gurson (1977).

Employing a yield function for porous metals with the normality flow rule,† the theory is compared with experimental data (Shipman *et al.*, 1975) for porous tungsten under hydrostatic compression and uniaxial strain compression. A special yield function used in this paper, in which the porosity is the only hardening parameter, gave reasonably good agreement for experimental data of a real porous metal in small deformation. It is known, however, that strain hardening of a porous solid results not only from the change of porosity but also from the strain hardening of the matrix material. The effect of strain hardening of matrix material will be included in the future work.

## 2. BASIC EQUATIONS

The basic equations of a rate-independent constitutive theory presented by Casey and Naghdi (1981, 1984a) and by Carroll (1987) are summarized here. It is assumed that the stress tensor‡ $s_{KL}$ is a function of the strain tensor $e_{KL}$ and a symmetric second-order plastic strain tensor $e^{\mathrm{p}}_{KL}$

$$s_{KL} = \hat{s}_{KL}(e_{MN}, e^{\mathrm{p}}_{MN}) \tag{1}$$

and that, for fixed valus of $e^{\mathrm{p}}_{KL}$, eqn (1) can be inverted to give

$$e_{KL} = \hat{e}_{KL}(s_{MN}, e^{\mathrm{p}}_{MN}). \tag{2}$$

It is also assumed that there exists a loading function $g$ in strain space such that for each value of $e^{\mathrm{p}}_{KL}$

$$g(e_{KL}, e^{\mathrm{p}}_{KL}) = 0 \tag{3}$$

defines an open region $\mathscr{E}$ of six-dimensional strain space (called the elastic region), with its boundary $\partial\mathscr{E}$ (called the yield surface). States $(e_{KL}, e^{\mathrm{p}}_{KL})$ with $g < 0$ are elastic and with $g = 0$ are elastic–plastic. The function $\hat{g}$, defined by

$$\hat{g} = \frac{\partial g}{\partial e_{KL}} \dot{e}_{KL} \tag{4}$$

affords strain space criteria of unloading ($\hat{g} < 0$), neutral loading ($\hat{g} = 0$), and loading ($\hat{g} > 0$) from a plastic state.

With the use of eqns (2) and (3), one obtains a corresponding load function $f$ in stress space, so that

$$f(s_{KL}, e^{\mathrm{p}}_{KL}) = g(e_{KL}, e^{\mathrm{p}}_{KL}). \tag{5}$$

This allows an elastic region $\mathscr{S}: f < 0$ and a yield surface $\partial\mathscr{S}: f = 0$ in stress space to be defined. The function $\hat{f}$ given by

$$\hat{f} = \frac{\partial f}{\partial s_{KL}} \dot{s}_{KL} \tag{6}$$

enables hardening, softening, and perfectly plastic behavior to be defined (Casey and Naghdi, 1981). As mentioned earlier, loading is defined by the condition $g = 0$, $\hat{g} > 0$ in strain space formulation. Strain hardening behavior of a material is characterized during loading by the sign of the function $\Phi = \hat{f}/\hat{g}$, so that the scalar function $\Phi$ may be positive

† Carroll and Carman (1985) carried out a check on the assumption of normality for porous solids using a finite element hollow sphere model. The assumption was plausible, at least for uniaxial strain and biaxial plane strain problems.

‡ A distinction between the Piola–Kirchhoff stress tensor or either of the Cauchy stress tensors is not necessary when only a small deformation is being considered.

(if the material is hardening), zero (if the material is behaving perfectly plastically), or negative (if the material is softening). It is noteworthy that the quotient $\hat{f}/\hat{g}$ is independent of rates, since $\hat{f}$ involves the time rate of the stress tensor and $\hat{g}$ the time rate of the strain tensor. It is also shown that (Casey and Naghdi, 1981), while during loading the yield surface in strain space is always moving outwards locally ($g = 0, \hat{g} > 0$), the corresponding yield surface in stress space may concurrently be moving outwards ($f = 0, \hat{f} > 0$), inwards ($f = 0, \hat{f} < 0$), or may be stationary ($f = 0, \hat{f} = 0$) depending on whether the material is hardening, softening, or exhibiting perfectly plastic behavior. The scalar function $\Phi$ also satisfies†

$$\Phi = \frac{\Gamma}{\Gamma+\Lambda} \tag{7}$$

where

$$\Lambda = \frac{\partial f}{\partial s_{KL}}\frac{\partial g}{\partial e_{KL}}, \quad \Gamma = -\frac{\partial f}{\partial s_{KL}}\frac{\partial f}{\partial e^{\mathrm{p}}_{KL}}, \quad \Gamma+\Lambda > 0. \tag{8}$$

For the present purpose, it is sufficient to consider a special case of eqn (1), i.e.

$$s_{KL} = \mathscr{C}_{KLMN}(e_{MN} - e^{\mathrm{p}}_{MN}) \tag{9}$$

where $\mathscr{C}_{KLMN}$ is the constant fourth-order elastic modulus tensor. Then, the constitutive equations for the rate of plastic strain $\dot{e}^{\mathrm{p}}_{KL}$ expressed as (see the development between eqns (36)–(42) in Casey and Naghdi (1981))

$$\dot{e}^{\mathrm{p}}_{KL} = \frac{\hat{g}}{\Gamma+\Lambda}\frac{\partial f}{\partial s_{KL}}. \tag{10}$$

## 3. SPECIAL CONSTITUTIVE EQUATIONS

It is convenient to decompose various tensors into their spherical and deviatoric parts. Thus, one can write

$$\tau_{KL} = s_{KL} - \bar{s}\delta_{KL}, \quad \gamma_{KL} = e_{KL} - \bar{e}\delta_{KL}, \quad \gamma^{\mathrm{p}}_{KL} = e^{\mathrm{p}}_{KL} - \bar{e}^{\mathrm{p}}\delta_{KL}$$
$$\bar{s} = \tfrac{1}{3}s_{KK}, \quad \bar{e} = \tfrac{1}{3}e_{KK}, \quad \bar{e}^{\mathrm{p}} = \tfrac{1}{3}e^{\mathrm{p}}_{KK}. \tag{11}$$

It is assumed that the matrix compressibility is negligible. The stress response function (9) is specified by the generalized Hooke's law

$$\tau_{KL} = 2\mu(\gamma_{KL} - \gamma^{\mathrm{p}}_{KL}), \quad \bar{s} = 3k(\bar{e} - \bar{e}^{\mathrm{p}}) \tag{12}$$

where $\mu$ and $k$ are the effective shear modulus and the effective bulk modulus for a porous metal, respectively. Since the matrix compressibility is negligible, the measure of the porosity $\phi$ ($= V_{\mathrm{p}}/V$) is given by (Carroll, 1980)

$$\phi = 1 - (1-\phi_0)\exp(v) \tag{13}$$

where $V$ and $V_{\mathrm{p}}$ denote the total volume and the pore volume, respectively, $v$ ($= -e_{KK}$) is the compressive volume strain, and $\phi_0$ the initial porosity. From the assumed smallness of strain porosity, eqn (13) can also be approximated by

$$\phi = 1 - (1-\phi_0)(1+v). \tag{14}$$

One now considers a special loading function of the form

† See eqn (4.13) in Casey and Naghdi (1984b).

$$f = \tfrac{1}{2}\tau_{KL}\tau_{KL} + \alpha\phi\bar{s}^2 - \tfrac{1}{3}(1-\phi)^n Y_s^2$$
$$g = 2\mu^2(\gamma_{KL}-\gamma_{KL}^p)(\gamma_{KL}-\gamma_{KL}^p) + \alpha\phi\{3k(\bar{e}-\bar{e}^p)\}^2 - \tfrac{1}{3}(1-\phi)^n Y_s^2 \tag{15}$$

where $\alpha$ and $n$ are constants and $Y_s$ is the initial yield strength of the solid material. In view of eqns (13) and (2), $\phi$ is a function of $s_{KL}$ and $e_{KL}^p$ in eqn $(15)_1$ and $e_{KL}$ in eqn $(15)_2$. Equation $(15)_2$ is obtained from eqn $(15)_1$ with the use of eqns (12). As the porosity becomes smaller, the contribution of mean normal stress becomes smaller and that of the yield strength becomes larger. The yield functions for porous solids which have been proposed by other researchers also have similar structures. If the material does not exhibit a significant hardening in small deformation, loading function $(15)_1$ in which the porosity is the only hardening parameter may be a reasonable one.

Use of eqns (8) and (15) gives

$$\frac{\partial f}{\partial s_{KL}} = \tau_{KL} + \left[\frac{2}{3}\alpha\phi\bar{s} + \frac{\alpha(1-\phi)\bar{s}^2}{3k} + \frac{n}{9k}(1-\phi)^n Y_s^2\right]\delta_{KL}$$

$$\frac{\partial g}{\partial e_{KL}} = 2\mu\tau_{KL} + \left[2\alpha k\phi\bar{s} + \alpha(1-\phi)\bar{s}^2 + \frac{n}{3}(1-\phi)^n Y_s^2\right]\delta_{KL}$$

$$\Gamma = -\left\{2\alpha\phi\bar{s} + \frac{\alpha(1-\phi)}{k}\bar{s}^2 + \frac{n}{3k}(1-\phi)^n Y_s^2\right\}\left\{\alpha\bar{s}^2(1-\phi) + \frac{n}{3}(1-\phi)^n Y_s^2\right\}$$

$$\Lambda = 2\mu\tau_{KL}\tau_{KL} + \left\{2\alpha\phi\bar{s} + \frac{\alpha(1-\phi)}{k}\bar{s}^2 + \frac{n}{3k}(1-\phi)^n Y_s^2\right\} \times \left\{2\alpha k\phi\bar{s} + \alpha(1-\phi)\bar{s}^2 + \frac{n}{3}(1-\phi)^n Y_s^2\right\}. \tag{16}$$

## 4. SPECIAL LOADING CONDITIONS

### 4.1. *Hydrostatic compression*

Hydrostatic compression of a porous metal by external pressure is considered. Adopting the notations $p = -\bar{s}$, $v = -3\bar{e}$, and $v^p = -3\bar{e}^p$, one has $\tau_{KL} = \gamma_{KL} = \gamma_{KL}^p = 0$ from spherical symmetry. Here $p$, $v$, and $v^p$ denote pressure, compressive volume strain, and compressive plastic volume strain, respectively. Loading function $(15)_1$ now reduces to the simplified form

$$f = \alpha\phi p^2 - \tfrac{1}{3}(1-\phi)^n Y_s^2 \tag{17}$$

and the constitutive equations, eqns (12) and (10), reduce to

$$p = k(v - v^p) \tag{18}$$

and

$$\dot{v}^p = \frac{[2\alpha k\phi p - \alpha(1-\phi)p^2 - n(1-\phi)^n Y_s^2/3]}{2\alpha k\phi p}\dot{v}. \tag{19}$$

### 4.2. *Uniaxial strain compression*

Uniaxial strain compression (a strain controlled test, i.e. $e_{11} \neq 0$ and $e_{22} = e_{33} = 0$) of a porous metal is now considered. Assuming that $s_{22} = s_{33}$ and $e_{22}^p = e_{33}^p$, one can write

$$\tau_{KL} = \tfrac{1}{3}(s_{11}-s_{22})b_{KL}, \quad \gamma_{KL} = \tfrac{1}{3}e_{11}b_{KL}, \quad \gamma_{KL}^p = \tfrac{1}{3}(e_{11}^p - e_{22}^p)b_{KL}$$
$$\bar{s} = \tfrac{1}{3}(s_{11}+2s_{22}), \quad \bar{e} = \tfrac{1}{3}e_{11}, \quad \bar{e}^p = \tfrac{1}{3}(e_{11}^p + 2e_{22}^p) \tag{20}$$

and

$$\phi = 1-(1-\phi_0)\exp(-e_{11}) \tag{21}$$

where

$$b_{KL} = \begin{bmatrix} 2 & 0 & 0 \\ 0 & -1 & 0 \\ 0 & 0 & -1 \end{bmatrix}. \tag{22}$$

Use of eqns (20) gives loading function $(15)_1$ in the form

$$f = \tfrac{1}{3}\tau^2 + \alpha\phi p^2 - \tfrac{1}{3}(1-\phi)^n Y_s^2 \tag{23}$$

and the constitutive equations, eqns (12) and (10), reduce to

$$s_{11} = \frac{4\mu}{3}(e_{11}-e_{11}^p+e_{22}^p)+k(e_{11}-e_{11}^p-2e_{22}^p)$$

$$s_{22} = -\frac{2\mu}{3}(e_{11}-e_{11}^p+e_{22}^p)+k(e_{11}-e_{11}^p-2e_{22}^p) \tag{24}$$

and

$$\dot{e}_{11}^p = [4\mu\tilde{\tau}+6\alpha\phi k\tilde{p}+3\alpha(1-\phi)\tilde{p}^2+n(1-\phi)^n Y_s^2]\left[2\tilde{\tau}+2\alpha\phi\tilde{p}+\frac{\alpha}{k}(1-\phi)\tilde{p}^2 + \frac{n}{3k}(1-\phi)^n Y_s^2\right]\dot{e}_{11}\Big/[12\mu\tilde{\tau}^2+18\alpha\phi\tilde{p}[2\alpha\phi k\tilde{p}+\alpha(1-\phi)\tilde{p}^2+n(1-\phi)^n Y_s^2/3]]$$

$$\dot{e}_{22}^p = [4\mu\tilde{\tau}+6\alpha\phi k\tilde{p}+3\alpha(1-\phi)\tilde{p}^2+n(1-\phi)^n Y_s^2]\left[-\tilde{\tau}+2\alpha\phi\tilde{p}+\frac{\alpha}{k}(1-\phi)\tilde{p}^2 + \frac{n}{3k}(1-\phi)^n Y_s^2\right]\dot{e}_{11}\Big/[12\mu\tilde{\tau}^2+18\alpha\phi\tilde{p}[2\alpha\phi k\tilde{p}+\alpha(1-\phi)\tilde{p}^2+n(1-\phi)^n Y_s^2/3]] \tag{25}$$

where

$$\tilde{p} = -p = (s_{11}+2s_{22})/3; \quad \tilde{\tau} = -\tau = s_{11}-s_{22}. \tag{26}$$

In eqns (26), $p$ and $\tau$ $(=-\sqrt{(\frac{3}{2}\tau_{KL}\tau_{KL})})$, respectively, denote compressive mean normal stress and deviatoric stress.

## 5. COMPARISON WITH EXPERIMENTAL DATA

The constitutive theory for porous metals, developed in previous sections, and the experimental data of porous tungsten obtained by Shipman *et al.* (1975), are now compared. Parameters $\alpha$ and $n$ in yield function $(15)_1$ are first determined from the initial yield surface of the experimental data (Shipman *et al.*, 1975). A non-linear regression method, e.g. BMDP statistical software (Jennrich, 1983) may be used to find the best estimate of parameters $\alpha$ and $n$. The average initial porosity of porous tungsten is $\phi_0 = 0.211$ (Shipman *et al.*, 1975) and the initial yield strength of solid tungsten is $Y_s = 0.965$ GPa (*Metals Handbook*, 1984). The porosity $\phi = \phi_1$ at the initial yield in eqn $(15)_1$ is obtained from the spherical model analysis (Carroll, 1980). Thus

$$\phi_1 = \frac{\phi_0}{1+(Y_s/2\mu_s)(1-\phi_0)} \tag{27}$$

where $Y_s$ and $\mu_s$ denote the initial yield strength and shear modulus of the solid material.†

† The value of $Y_s/2\mu_s = 0.005$ was used.

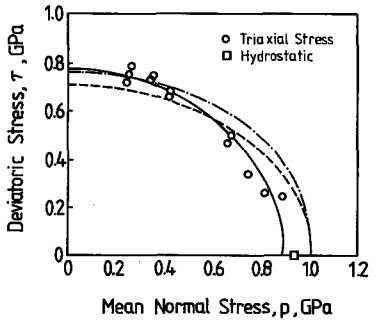


Fig. 1. Comparison of the experimental data of the initial yield from various triaxial loading tests for porous tungsten (Shipman *et al.*, 1975) (data points) with the initial yield surface from eqn $(15)_1$ (solid curve), with $\alpha = 1.2$, $n = 1.9$, and $Y_s = 0.965$ GPa. The initial yield surfaces of Green (dashed curve) and of Gurson (dash-dot curve) are also shown.

Figure 1 compares the experimental data (data points) of initial yield from various loading conditions for porous tungsten, obtained by Shipman *et al.* (1975) with the initial yield surface obtained from eqn $(15)_1$ (solid curve), with $\alpha = 1.2$ and $n = 1.9$ and the initial yield surfaces of Green (dashed curve) and of Gurson (dash-dot curve). The yield functions of Green (1972) and Gurson (1977) are written in the present notations respectively as

$$f = \tfrac{1}{2}\tau_{KL}\tau_{KL} + 3a^2(\phi)\bar{s}^2 - \tfrac{1}{3}b^2(\phi)Y_s^2 \tag{28}$$

and

$$f = \tfrac{1}{2}\tau_{KL}\tau_{KL} + \tfrac{2}{3}\phi Y_s^2 \cosh\left(\frac{3\bar{s}}{2Y_s}\right) - \tfrac{1}{3}(1+\phi^2)Y_s^2 \tag{29}$$

where

$$a(\phi) = \frac{b(\phi)}{2\ln(\phi)}; \quad b(\phi) = \frac{3(1-\phi^{1/3})}{3-2\phi^{1/4}}. \tag{30}$$

It is observed that the initial yield surface obtained from eqn $(15)_1$ gives a better agreement for the experimental data of porous tungsten, compared to the initial yield surfaces of Green (1972) and of Gurson (1977). The yield functions of Green (1972) and Gurson (1977) are obtained from the hollow sphere model, with a rigid–perfectly plastic material. The hollow sphere model, however, overestimates the compacting pressure in the elastic region and in the small plastic region, because in these regions there still exist aspherical pores and flat microcracks which are easier to deform than spherical pores (Schatz, 1976).

Figure 2 compares a theoretical hydrostatic compression curve for porous tungsten with experimental data (Shipman *et al.*, 1975). The theoretical curve is calculated using eqns (18) and (19), with the material constants obtained in Fig. 1. The effective bulk modulus $k = 110$ GPa is used by comparing theory and experiment in the elastic range of the pressure vs volume strain data.

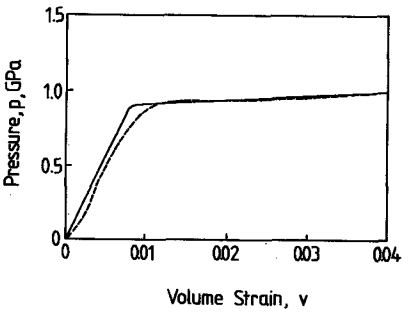


Fig. 2. Comparison of an experimental pressure vs volume strain curve (dashed curve) during hydrostatic compression (Shipman *et al.*, 1975) with the theoretical hydrostatic curve calculated from eqns (18) and (19).

Table 1. Theoretical and experimental porosity during hydrostatic compression

| $P$ (GPa) | $v$ | Experimental $\phi$ | Theoretical $\phi$ |
|---|---|---|---|
| 0 | 0 | 0.2107 | 0.2107 |
| 0.1 | 0.0016 | 0.2095 | 0.2094 |
| 0.2 | 0.0026 | 0.2089 | 0.2086 |
| 0.3 | 0.0033 | 0.2082 | 0.2081 |
| 0.4 | 0.0041 | 0.2076 | 0.2075 |
| 0.5 | 0.0051 | 0.2070 | 0.2067 |
| 0.6 | 0.0061 | 0.2064 | 0.2059 |
| 0.7 | 0.0072 | 0.2051 | 0.2050 |
| 0.8 | 0.0086 | 0.2038 | 0.2039 |
| 0.875 | 0.0098 | 0.2032 | 0.2030 |
| 0.9 | 0.0106 | 0.2026 | 0.2023 |
| 0.925 | 0.0113 | 0.2020 | 0.2018 |
| 0.95 | 0.0240 | 0.1916 | 0.1918 |
| 0.975 | 0.0312 | 0.1857 | 0.1861 |
| 1.0 | 0.0403 | 0.1776 | 0.1789 |

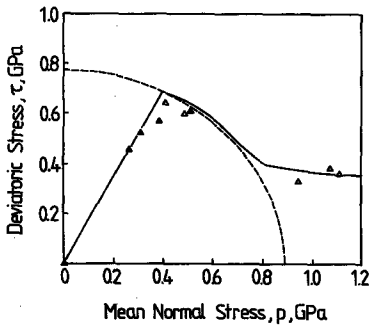


Fig. 3. Comparison of a theoretical uniaxial strain compression behavior (solid curve) with the experimental data (△) from Shipman *et al.* (1975) on the deviatoric stress vs mean normal stress relation for porous tungsten. The initial yield surface is also shown (dashed curve).

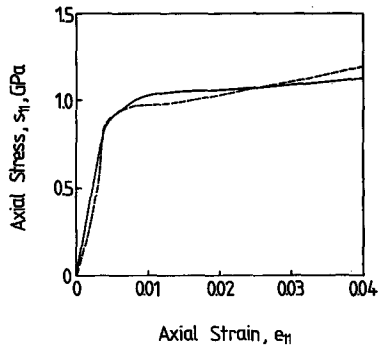


Fig. 4. Comparison of a theoretical uniaxial strain compression behavior (solid curve) with experimental data (dashed curve) from Shipman *et al.* (1975) on the axial stress vs axial strain relation for porous tungsten.

Table 1 shows theoretical and experimental porosity for porous tungsen during hydrostatic compression. The agreement between theory and experiment for hydrostatic compression is reasonably good.

Figure 3 compares a theoretical stress path (solid curve) of uniaxial strain compression for porous tungsten with the experimental data (△) (Shipman *et al.*, 1975). The initial yield surface is also shown (dashed curve). The theoretical stress path is calculated using eqns (24) and (25). The effective shear modulus $\mu = 95$ GPa is used by comparing theory and experiment in the elastic range of the stress path. By using the effective elastic moduli $k$ and $\mu$, which were chosen respectively from elastic regions of Figs 2 and 3, reasonably good agreements were obtained between theoretical predictions and experimental data in plastic regions of Figs 2 and 3. Moreover, Fig. 4 shows the predictive capabilities of theory by using

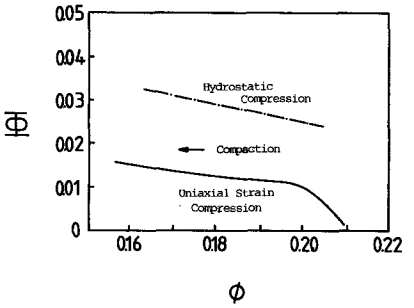


Fig. 5. Strain hardening responses of porous tungsten for hydrostatic compression (dashed curve) and uniaxial strain compression (solid curve). These curves are calculated using eqns (7) and (8).

material constants obtained in Figs 1–3. Figure 4 compares a theoretical axial stress vs axial strain curve (solid curve) of uniaxial strain compression for porous tungsten and the experimental data (dashed curve). The theoretical curve is calculated using eqns (24) and (25). The agreement is good up to an axial strain of 0.03, but the predicted axial stress at higher axial strains are lower than the measured values. It appears that the strain hardening of porous tungsten at a higher stain level may be greater than that predicted by yield function $(15)_1$. Figure 5 shows strain hardening behaviors of porous tungsten. These curves are calculated for hydrostatic compression (dashed curve) and uniaxial strain compression (solid curve) by using eqns (7) and (8). It is observed that a porous metal exhibits strain hardening ($\Phi > 0$) during hydrostatic compression and uniaxial strain compression. The change of porosity $\Delta\phi$ is negative† during compression and the change of the rate-independent quotient $\Delta\Phi$ is positive when a material exhibits strain hardening. Numerical results also show that $\partial\Phi/\partial\phi$ is negative which means that a porous metal exhibits strain hardening during hydrostatic compression and uniaxial strain compression.

*Acknowledgements*—Part of this work was carried out while the author was a postdoctoral fellow at the Department of Mechanical Engineering, University of California, Berkeley. The financial support from Professor M. M. Carroll and his helpful discussions are gratefully acknowledged. This work was also supported by Pohang Institute of Science and Technology.

## REFERENCES

Carroll, M. M. (1980). Mechanical response of fluid-saturated porous materials. *Proc. 15th Int. Cong. Theoret. Appl. Mech.* (Edited by F. P. J. Rimrott and B. Tabarrok), p. 251. North-Holland, New York.

Carroll, M. M. (1987). A rate-independent constitutive theory for finite elastic–plastic deformation. *J. Appl. Mech.* **54,** 15.

Carroll, M. M. and Carman, R. A. (1985). Discussion of influence of yield surface curvature on flow localization in dilatant plasticity, by M. E. Mear and J. W. Hutchinson. *Mech. Mater.* **4,** 409.

Carroll, M. M. and Holt, A. C. (1972). Static and dynamic pore-collapse relations for ductile porous solids. *J. Appl. Phys.* **44,** 1626.

Carroll, M. M. and Holt, A. C. (1973). Steady waves in ductile porous solids. *J. Appl. Phys.* **44,** 4388.

Carroll, M. M. and Kim, K. T. (1984). Pressure–density equations for porous metals and metal powders. *Powder Metall.* **27,** 153.

Casey, J. and Naghdi, P. M. (1981). On the characterization of strain hardening in plasticity. *J. Appl. Mech.* **48,** 285.

Casey, J. and Naghdi, P. M. (1983). A remark on the definition of hardening, softening, and perfectly plastic behavior. *Acta Mech.* **48,** 91.

Casey, J. and Naghdi, P. M. (1984a). Further constitutive results in finite plasticity. *Q. J. Mech. Appl. Math.* **37,** 231.

Casey, J. and Naghdi, P. M. (1984b). Strain-hardening response of elastic–plastic materials. In *Mechanics of Engineering Materials* (Edited by C. S. Desai and R. H. Gallagher), Chap. 4. Wiley, New York.

Curran, J. H. and Carroll, M. M. (1979). Shear stress enhancement of void compaction. *J. Geophys. Res.* **84,** 1105.

de Boer, R. and Kowalski, S. J. (1983). A plasticity theory for fluid-saturated porous solids. *Int. J. Engng Sci.* **21,** 1343.

Green, A. E. and Naghdi, P. M. (1965). A general theory of an elastic–plastic continuum. *Archs Ration. Mech. Analysis* **18,** 251.

† During compression the porosity $\phi$ becomes smaller as compressive volume strain $v$ becomes larger (see eqn (13)).

Green, R. J. (1972). A plasticity theory for porous solids. *Int. J. Mech. Sci.* **14,** 215.
Green, A. E. and Naghdi, P. M. (1966). A thermodynamic development of elastic–plastic continua. *Proc. IUTAM Symp. on Irreversible Aspects of Continuum Mech. and Transfer of Physical Characteristics in Moving Fluids* (Edited by H. Parkus and L. I. Sedov), p. 25. Springer, Berlin.
Gurson, A. L. (1977). Continuum theory of ductile rupture by void nucleation and growth—Part I. Yield criteria and flow rules for porous ductile media. *J. Engng Mater. Technol.* **99,** 2.
Jennrich, R. (1983). P3R—Nonlinear regression. In *BMDP Statistical Software* (Edited by W. J. Dixon), p. 289. University of California Press.
Johnson, J. N. and Green, S. J. (1976). Mechanical response of porous media subject to static loads. In *The Effects of Voids on Material Deformation* (Edited by S. C. Cowin and M. M. Carroll), AMD-16, p. 93. ASME, New York.
Kim, K. T. and Carroll, M. M. (1987). Compaction equations for strain hardening porous materials. *Int. J. Plasticity* **3,** 63.
Kuhn, H. A. and Downey, C. L. (1971). Deformation characteristics and plastic theory of sintered powder materials. *Int. J. Powder Metall.* **7,** 15.
Mackenzie, J. K. (1950). The elastic constants of a solid containing spherical holes. *Proc. Phys. Soc.* **B63,** 2.
*Metals Handbook* (1984). 9th Edn, Vol. 7, p. 476. American Society for Metals, Ohio.
Naghdi, P. M. and Trapp, J. A. (1975a). The significance of formulating plasticity theory with reference to loading surfaces in strain space. *Int. J. Engng Sci.* **13,** 785.
Naghdi, P. M. and Trapp, J. A. (1975b). Restrictions on constitutive equations of finitely deformed elastic–plastic materials. *Q. J. Mech. Appl. Math.* **28,** 25.
Schatz, J. F. (1976). Models of inelastic volume deformation for porous geologic materials. In *The Effects of Voids on Material Deformation* (Edited by S. C. Cowin and M. M. Carroll), AMD-16, p. 141. ASME, New York.
Shima, S. and Oyane, M. (1976). Plasticity theory for porous metals. *Int. J. Mech. Sci.* **18,** 285.
Shipman, F. H., Abou-Sayed, A. S. and Jones, A. H. (1975). Physical and mechanical characterization of a porous tungsten. Report No. 75-59, Terra-Tek Inc., Salt Lake City, Utah.
Torre, C. (1948). Theorie und Verhalten zusammengepreßteer Pulver. *Berg- u. Hüttenm. Mh.* **93,** 62.